Photonic Integration for Low Size, Weight, and Power (SWaP) Remote Gas Spectroscopy

Victoria Rosborough[1*], Joseph Fridlander[1], Fengqiao Sang[1], Fabrizio Gambini[2,3], Simone Tommaso Šuran Brunelli[1], Jeffrey R. Chen[4], Stephan Kawa[4], Kenji Numata[4], Mark Stephen[4], Larry Coldren[1], Jonathan Klamkin[1]

[1]*Electrical and Computer Engineering Department, University of California Santa Barbara, Santa Barbara, CA 93106 USA*
[2]*University of Maryland Baltimore County, Baltimore, MD 21250 USA*
[3]*NASA Goddard Space Flight Center / CRESST II, Greenbelt, MD 20771 USA*
[4]*NASA Goddard Space Flight Center, Greenbelt, MD 20771 USA*
**rosborough@ucsb.edu*

Abstract: Subsystem operation of a photonic integrated circuit for low size, weight, and power remote gas sensing was demonstrated. Precision lidar system specifications for laser tuning, photodiode bandwidth and pulse extinction ratio were satisfied. A twentyfold improvement in long-term laser frequency stability was achieved. © 2021 The Author(s)

OCIS codes: (250.5300) Photonic integrated circuits; (280.3640) Lidar

1. Introduction

Active remote sensing of CO_2 would provide improved temporal and spatial resolution compared to the passive spectrometer measurement systems now in use [1]. A candidate integrated path differential absorption lidar system for NASA's Active Sensing of CO_2 Emissions over Nights, Days and Seasons (ASCENDS) mission was developed with commercial-off-the-shelf components at NASA Goddard Space Flight Center [2]. Using integrated photonics, an equivalent lidar system can be realized at a fraction of the size, weight, and power consumption (SWaP) [3]. A photonic integrated circuit (PIC) remote sensing module would not only be more compact and cost effective, but potentially more robust due to a decrease in the number of bulk optical connectors. In this work, we present an indium phosphide (InP) PIC for remote CO_2 sensing that translates the ASCENDS design for use in small form-factor platforms.

2. PIC Architecture and Fabrication

Figure 1 shows a photo of the fabricated PIC and illustrates the lidar operation. A master laser is stabilized to the 1572.335-nm absorption line center (ν_0) of CO_2 using a frequency modulation technique [4]. Part of the light from the master laser goes to an integrated phase modulator and is then coupled off-chip to a CO_2 reference cell. A beat note detected at the output of the CO_2 cell results in an error signal that provides feedback to the phase section of the master laser. A slave laser is offset-locked to the master laser via an optical phase locked loop (OPLL). The slave laser frequency is stepped through a discrete set of values to sample the atmospheric absorption line. After the slave laser steps to a new frequency, an amplitude modulator carves a high extinction ratio (>40 dB) pulse, which is coupled off-chip to an erbium doped fiber amplifier (EDFA). The 1-μs pulses are separated by 133 μs to eliminate crosstalk from cloud scattering [5].

An InP-based material system was chosen for the PIC because it is mature, exhibits a compatible wavelength range, and provides monolithic integration of both active and passive components. The PIC was fabricated at the UC Santa Barbara Nanofabrication Facility using an offset quantum well (OQW) epitaxial design that allows the gain material to be selectively etched away in the passive regions.

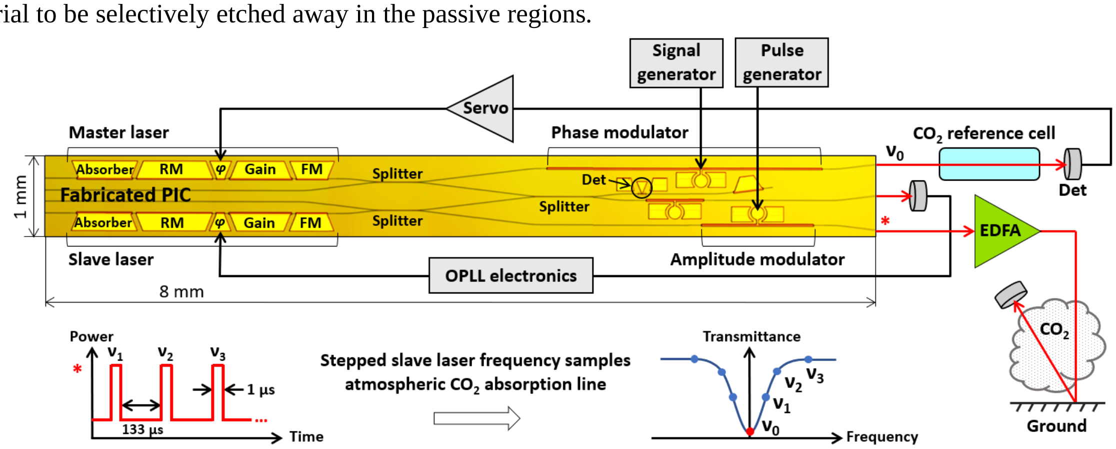

Figure 1. PIC and LIDAR system architecture for CO_2 monitoring. RM = rear mirror; FM = front mirror; φ = phase section; Det = detector.

3. Subsystem Characterization

We have demonstrated independent operation of each of the subsystems described above. Figure 2(a) shows the reference cell gas absorption overlaid with the error signal used to lock the master laser to the CO_2 absorption line. The error signal is proportional to the deviation from the line center. Fig. 2(b) plots the beat note used to characterize the master laser frequency stability. With feedback to the master laser, the peak-to-peak frequency deviations improved from 151 MHz to 7.6 MHz over 10 minutes for one-second gate times. The standard deviation in the frequency also experiences a twentyfold improvement from 30.2 MHz without feedback to 1.54 MHz with feedback. Figure 2(c) illustrates the slave laser frequency stability with and without the OPLL over 10 minutes for one-second gate times. For a programmed frequency offset of 2 GHz, the standard deviation in the slave laser frequency was 5.08 MHz and the average frequency offset from the master laser was 2.000087 GHz. Plotted in Fig. 2(d) is the frequency stepping of the slave laser from 1 to 15 GHz offset from the master laser frequency of 1572.335 nm. An integrated photodetector was included in the PIC (circled in Fig. 1) for on-chip detection of the beat note between the master and slave laser for the OPLL. Due to a fabrication defect, an off-chip detector was needed to demonstrate the slave laser locking. However, characterization of other integrated photodiodes did show the desired 15 GHz 3-dB bandwidth operation as shown in Fig. 2(e). Finally, a 1-μs pulse with an extinction ratio of at least 40 dB at the output of the amplitude modulator is shown in Fig. 2(f). The pulse extinction ratio was estimated using a DC measurement because the power level in the off state was below the photodiode noise floor.

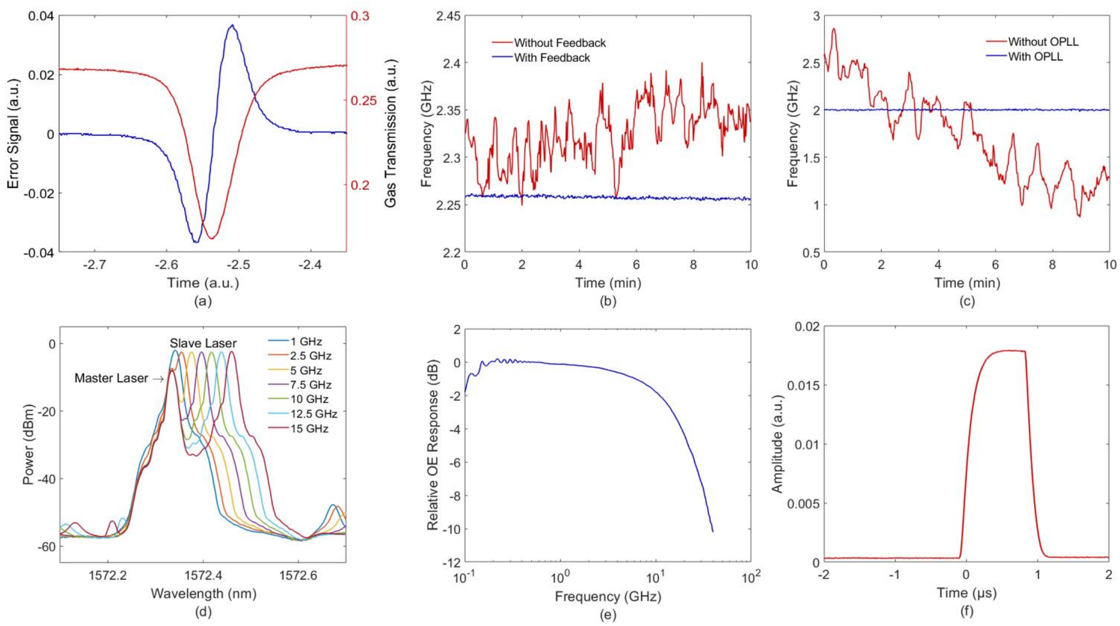

Figure 2. (a) error signal and gas absorption; (b) master laser frequency stability; (c) OPLL beat note for slave laser offset 2 GHz from master laser; (d) overlaid master and slave laser spectra for slave laser offsets of 1-15 GHz; (e) integrated photodiode response showing 15 GHz 3-dB bandwidth; (f) 1-μs pulse from amplitude modulator.

4. Conclusion

An InP PIC for low-SWaP CO_2 lidar was designed, fabricated, and evaluated for system level specifications. Integrated master and slave lasers were successfully stabilized for slave laser frequency offsets of up to 15 GHz. An integrated pulse carver achieved a 40-dB extinction ratio. Future work includes packaging with compact electronic control boards and demonstration of CO_2 sensing.

5. Acknowledgements

The authors acknowledge NASA for support through the ROSES Advanced Component Technology program. A portion of this work was performed in the UCSB Nanofabrication Facility.

6. References

[1] S. M. R. Crowell, et al., “On the ability of space-based passive and active remote sensing observations of CO2 to detect flux perturbations to the carbon cycle,” *J. Geophysical Research: Atmospheres*, **123**, 1460—1477, (2018).

[2] K. Numata, et al., “Precision and fast wavelength tuning of a dynamically phase-locked widely-tunable laser,” *Optics Express*, **20** (13) 14234—14243 (2012).

[3] J. Fridlander, et al., “Photonic integrated circuits for precision spectroscopy,” presented at CLEO conf., SF30.3, (2020).

[4] G.C. Bjorklund, *Optics Letters*, **5** (1) 15-17 (1980).

[5] K. Numata, et al., “Frequency stabilization of distributed-feedback laser diodes at 1572 nm for lidar measurements of atmospheric carbon dioxide,” *Applied Optics*, **50** (7) 1047—1056 (2011)